THE JOURNAL OF BIOLOGICAL CHEMISTRY
Vol. 278, No. 10, Issue of March 7, pp. 8826–8836, 2003

Printed in U.S.A.

Highly Coordinated Gene Regulation in Mouse Skeletal Muscle Regeneration*[S]

Received for publication, September 26, 2002, and in revised form, December 2, 2002
Published, JBC Papers in Press, December 10, 2002, DOI 10.1074/jbc.M209879200

Zhen Yan‡§, Sangdun Choi¶, Xuebin Liu‖, Mei Zhang‡, Jeoffrey J. Schageman‖, Sun Young Lee¶, Rebecca Hart¶, Ling Lin‖, Frederick A. Thurmond‖, and R. Sanders Williams‡

From the ‡Division of Cardiology, Department of Medicine, Duke University Medical Center, Durham, North Carolina 27710, the ¶Division of Biology, California Institute of Technology, Pasadena, California 91125, and the ‖Department of Internal Medicine, University of Texas Southwestern Medical Center, Dallas, Texas 75390

Mammalian skeletal muscles are capable of regeneration after injury. Quiescent satellite cells are activated to reenter the cell cycle and to differentiate for repair, recapitulating features of myogenesis during embryonic development. To understand better the molecular mechanism involved in this process *in vivo*, we employed high density cDNA microarrays for gene expression profiling in mouse tibialis anterior muscles after a cardiotoxin injection. Among 16,267 gene elements surveyed, 3,532 elements showed at least a 2.5-fold change at one or more time points during a 14-day time course. Hierarchical cluster analysis and semiquantitative reverse transcription-PCR showed induction of genes important for cell cycle control and DNA replication during the early phase of muscle regeneration. Subsequently, genes for myogenic regulatory factors, a group of imprinted genes and genes with functions to inhibit cell cycle progression and promote myogenic differentiation, were induced when myogenic stem cells started to differentiate. Induction of a majority of these genes, including E2f1 and E2f2, was abolished in muscles lacking satellite cell activity after gamma radiation. Regeneration was severely compromised in E2f1 null mice but not affected in E2f2 null mice. This study identifies novel genes potentially important for muscle regeneration and reveals highly coordinated myogenic cell proliferation and differentiation programs in adult skeletal muscle regeneration *in vivo*.

Skeletal muscles are damaged and repaired repeatedly throughout life. Muscle regeneration maintains locomotor function during aging and delays the appearance of clinical symptoms in neuromuscular diseases, such as Duchenne muscular dystrophy (1, 2). This capacity for tissue repair is conferred by satellite cells located between the basal lamina and the sarcolemma of mature myofibers (3, 4). Upon injury, satellite cells reenter the cell cycle, proliferate, and then exit the cell cycle either to renew the quiescent satellite cell pool or to differentiate into mature myofibers (5). Understanding the molecular mechanism by which satellite cell activity is regulated could promote development of novel countermeasures to enhance muscle performance that is compromised by diseases or aging.

Both the cell proliferation and differentiation programs are essential for myogenesis. Mammalian cells escape from quiescence (G_0) and enter the cell cycle by activating the Cdk[1]/Rb/E2f signaling pathway (6, 7). In general, mitogen stimulation induces expression and assembly of the G_1 cyclin-dependent kinases (Cdks) (8, 9). Activation of Cdks causes phosphorylation of the retinoblastoma protein (Rb) (10, 11), leading to increased activities of a subset of E2f transcription factors (E2fs) (12) and up-regulation of a variety of E2f-responsive genes encoding proteins directly involved in DNA replication and cell cycle progression (13, 14). On the other hand, myogenic differentiation is controlled by interactions of a network of myogenic transcription factors (15). Studies of myogenesis during embryonic development and in cultured myogenic cell lines have provided much insight into the functional role of these transcription factors (16–22). Briefly, paired box proteins (Pax3 and Pax7) are involved in myogenic cell lineage determination and specification (21, 23, 24), whereas primary basic helix-loop-helix myogenic regulatory factors (MRFs), MyoD and Myf5 (25, 26), and secondary MRFs, myogenin and MRF4 (27, 28), function downstream in terminal differentiation. MADS box transcription factors, such as myocyte enhancer factor 2, cooperate with MRFs in muscle-specific gene expression (29, 30). However, the functional roles of these regulatory proteins in adult skeletal muscle have not been well defined. Several animal models of muscle regeneration have been described, but there has not been a comprehensive analysis of gene regulation in any model. In this study, we have taken advantage of high density cDNA microarray to assess global gene expression followed by detailed semiquantitative reverse transcription (RT)-PCR analysis in a mouse skeletal muscle regeneration model. Expression of some genes directly related to cell cycle control and myogenic differentiation was compared in the presence and absence of satellite cell activities. We have identified genes previously unknown to be regulated during skeletal muscle regeneration. We have also uncovered differential functional roles of E2f1 and E2f2 *in vivo* using mice with targeted mutations.

* This work was supported by American Heart Association Grant 0130261N (to Z. Y.) and National Institutes of Health Grant AR40849 (to R. S. W.). The costs of publication of this article were defrayed in part by the payment of page charges. This article must therefore be hereby marked "*advertisement*" in accordance with 18 U.S.C. Section 1734 solely to indicate this fact.

[S] The on-line version of this article (available at http://www.jbc.org) contains the self-organization map and functional groups.

§ To whom correspondence should be addressed: Division of Cardiology, Dept. of Medicine, Duke University Medical Center, 201C MSRB, Research Dr., MC 2635, Durham, NC 27710. Tel.: 919-668-5579; Fax: 919-668-5392; E-mail: zhen.yan@duke.edu.

[1] The abbreviations used are: Cdk(s), cyclin-dependent kinase(s); BrdUrd, bromodeoxyuridine; Gas, growth arrest-specific; H&E, hematoxylin and eosin; Mcmd, minichromosome maintenance deficient; MOPS, 4-morpholinepropanesulfonic acid; MRF(s), myogenic regulatory factor(s); Orc, origin recognition complex; Pax, paired box; PBS, phosphate-buffered saline; Rb, retinoblastoma; RT, reverse transcription; Shh, sonic hedgehog; TA, tibialis anterior.

EXPERIMENTAL PROCEDURES

Muscle Injury Model—We modified a previously described muscle injury model (22) by injecting cardiotoxin into the tibialis anterior (TA) muscles of 6-week-old male C57BL/6 mice (Harlen). The muscles were harvested at various times (1, 2, 3, 5, 10, or 14 days) after injection. Uninjected TA muscles were used as control. 6 h before muscle harvesting, 500 mg/kg bromodeoxyuridine (BrdUrd) was injected intraperitoneally to label DNA-replicating nuclei. The left TA muscle was harvested, fixed in 4% paraformaldehyde, frozen or embedded in paraffin, sectioned, and stained with hematoxylin and eosin (H&E) or antibodies against various antigens. Total RNA was isolated from the right TA muscle using TriPure® kit (Roche Molecular Biochemicals). To assess the contribution of satellite cell activities in global gene expression, we injected cardiotoxin into TA muscles that had been subjected to 2,200 rads of gamma radiation (31) 24 h earlier. To determine whether induced expression of E2f1 or E2f2 is essential for injury-induced muscle regeneration, cardiotoxin was injected in TA muscles in mice with targeted mutation of E2f1 (Jackson Laboratory) or E2f2 allele (kind gifts from J. R. Nevins).

Indirect Immunofluorescence—8-μm frozen or paraffin-embedded muscle sections were permeabilized in 0.3% Triton X-100 and PBS, blocked with normal goat serum, and incubated overnight at 4 °C with rabbit anti-MyoD antibody (1:50, Santa Cruz), rat anti-Mac-1 (1:400, Serotec), or rat anti-ag 7/4 (1:400, Serotec) in 5% normal goat serum and PBS. The sections were incubated with fluorescein isothiocyanate-conjugated secondary antibody (1:50, Jackson Laboratory) in 5% normal goat serum and PBS for 30 min at room temperature. To detect BrdUrd incorporation, the sections were then fixed for 10 min in 2% formaldehyde on ice and treated with 2 N HCl for 60 min at 37 °C to denature the DNA followed by neutralization in 0.1 M borate buffer (pH 8.5). The sections were then permeabilized in 0.3% Triton X-100 and PBS and blocked with 1.5% normal horse serum and PBS and incubated overnight at 4 °C with mouse monoclonal anti-BrdUrd antibodies (1:25, Roche) in 0.1% bovine serum albumin and PBS followed by an incubation with biotinylated horse anti-mouse IgG (1:200, Dako) in 1% normal horse serum and PBS. The biotinylated IgG was detected by application of fluorescein isothiocyanate and streptavidin (1:50, Vector) and examined under epifluorescent or confocal microscope.

Transmission Electron Microscopy—TA muscles were fixed in a solution containing 2.5% glutaldehyde, 137 mM NaCl, 2 mM $CaCl_2$, 4 mM KCl, 100 mM MOPS (pH 7.4) for 24 h, rinsed in the fixation solution lacking glutaldehyde for 24 h, treated with 1% osmium tetroxide in 100 mM $C_2H_6AsO_2Na$ (cacodylate) for 2 h, stained with 0.5% uranyl acetate for 2 h, dehydrated in ethanol, and embedded in Spurr's resin. Thin sections were cut, collected on 400-mesh copper grids, and stained with uranyl acetate and lead citrate. Microscopy was carried out using a JEOL 1200 EX electron microscope at 80 kV.

RNA Isolation and DNA Microarray—A National Institute on Aging mouse cDNA chip (16,000 bytes) was used for the microarray analysis. PCR products from cDNA clones prepared by the Caltech Genome Research Laboratory (date.tree.caltech.edu/local_clones.html) were spotted onto CMT-GAPS-coated slides (Corning). Probes for microarray hybridization were generated using 5 μg of pooled muscle total RNA from five mice of the same time point. The RNA was first annealed with 100 pmol of T7-$(dT)_{24}$ primer (5′-GGCCAGTGAATTGTAATACGACTCACTATAGGGAGGCGG-$(dT)_{24}$-3′) in 12 μl at 70 °C for 10 min. The first strand cDNA was synthesized at 42 °C for 1 h in the first strand cDNA buffer containing 50 mM Tris (pH 8.3), 75 mM KCl, 3 mM $MgCl_2$, 10 mM dithiothreitol, 0.5 mM dNTP, and 10 units/μl Superscript II reverse transcriptase (Invitrogen). The second strand cDNA was synthesized at 16 °C for 2 h in the second strand cDNA buffer containing 20 mM Tris (pH 6.9), 90 mM KCl, 4.6 mM $MgCl_2$, 0.15 mM NAD, 10 mM $(NH_4)_2SO_4$, 0.2 mM dNTP, 0.07 unit/μl *Escherichia coli* DNA ligase (New England Biolabs), 0.27 unit/μl *E. coli* DNA polymerase I (New England Biolabs), and 0.013 unit/μl RNase H (Invitrogen). T4 DNA Polymerase (20 units, Invitrogen) was added and incubated at 16 °C for 5 min. To stop the reaction, 7.5 μl of 1 M NaOH and 2 mM EDTA (pH 8.0) was added, and the sample was heated at 65 °C for 10 min. The cDNA was extracted with phenol:chloroform:isoamyl alcohol (25:24:1) and precipitated with ammonium acetate and ethanol. *In vitro* transcription was carried out using a T7 Megascript kit (Ambion). To generate a Cy3- or Cy5-labeled probe, 10 μg of amplified antisense RNA and 6 μg of random hexamer primers were annealed in 14 μl at 70 °C for 10 min followed by incubation at 42 °C for 2 h in 50 mM Tris (pH 8.3), 75 mM KCl, 3 mM $MgCl_2$, 10 mM dithiothreitol, 10 μM dATP/dCTP/dGTP, 4 μM dTTP, 13.3 units/μl Superscript II reverse transcriptase (Invitrogen), and 3 μl Cy5 or Cy3 dUTP. The probes were purified by filtering through Microcon-30 filters (Millipore) before hybridization at 42 °C in a water bath overnight according to the instructions for CMT-GAPS-coated slides. The slides were scanned with a GenePix 4000A scanner (Axon Instruments) and analyzed using the GENEPIX PRO 3.0 (Axon Instruments).

Microarray Data Analysis—The raw data were normalized using a total intensity normalization method under the assumption that the total quantities of messages from both channels should be the same. Briefly, the average fold difference of all elements of the array was calculated and used as a normalization factor. This normalization factor was then used to adjust the fold for each gene in the array. We then eliminated spots that had median intensities less than the mean plus three times S.D. of the background Cy3 or Cy5 intensity. Once the normalized data were obtained and lower than background data points were removed, we processed the data further by removing any gene element that had not shown a change >2.5-fold at any time point. This cutoff level was set after we repeatedly tested the reproducibility of the microarray hybridization and found an average of only 10 gene elements with changes greater than 2.5-fold (maximal change of 2.8-fold) among 16,267 elements assayed (0.061%) when unstimulated control samples were compared (not shown). For clustering analysis, we converted the Cy5:Cy3 ratio to a log ratio (base 2), analyzed with GeneCluster 2.0 available at www-genome.wi.mit.edu, and generated a 4 × 4 self-organization map (32).

Semiquantitative RT-PCR—To confirm the microarray findings and to survey additional genes pertinent to satellite cell proliferation and differentiation, semiquantitative RT-PCR analysis was performed as described (22). Each data point was normalized by the abundance of glyceraldhyde-3-phosphate dehydrogenase mRNA and expressed as a log2 ratio to the uninjected control in the randomly preassigned time course group. PCR primer pairs were designed using a Primer3 search engine at www-genome.wi.mit.edu. The screened genes and the oligonucleotide primer pairs used for each of the genes in this study corresponded to the following nucleotides: glyceraldhyde-3-phosphate dehydrogenase, 114–136 and 403–383 (NM_008084); cell division cycle 6 homolog (*Saccharomyces cerevisiae*) (*Cdc6*), 203–224 and 927–907 (NM_011799); origin recognition complex, subunit 1 homolog (*S. cerevisiae*) (*Orc1*), 866–885 and 1238–1219 (NM_011015); *Orc2*, 2381–2400 and 2780–2761 (NM_008765); minichromosome maintenance-deficient 2 homolog (*S. cerevisiae*) (*Mcmd2*), 2580–2599 and 2903–2884 (NM_008564); *Mcmd3*, 1445–1464 and 1866–1847 (X62154); *E2f1*, 2030–2050 and 2147–2128 (L21973); E2f2, 8–27 and 140–121 (AA791874); *E2f3*, 403–422 and 753–733 (AF015948); *E2f4*, 471–490 and 705–686 (AA050824); *E2f5*, 441–459 and 744–725 (X86925); *E2f6*, 42–61 and 239–220 (AW211063); DRTF-polypeptide-1 (*DP1*), 422–441 and 868–849 (X72310); protein-regulating cell cycle transcription factor DRTF1/E2f (*DP3*), 867–887 and 1204–1185 (S79780); *Rb*, 1608–1627 and 2089–2068 (M26391); *p130*, 1882–2003 and 2272–2251 (U50850); *p107*, 1801–1820 and 2255–2236 (U27177); cyclin D1, 183–203 and 511–481 (NM_007631); cyclin D2, 732–751 and 1065–1045 (NM_009829); cyclin D3, 981–200 and 1326–1307 (NM_007632); cyclin E, 858–879 and 1164–1142 (NM_007633); cyclin E2, 52–71 and 423–403 (NM_009830); cyclin A2, 1002–1022 and 1325–1305 (NM_009828); cyclin B, 368–387 and 844–825 (X58708); *Pax3*, 244–263 and 629–610 (NM_008781); Pax7, 126–145 and 450–431 (U20792); MyoD, 671–690 and 1161–1139 (M84918); myogenin (Myog), 470–492 and 850–830 (D90156); Myf5, 504–528 and 761–738 (NM_008656); myogenic factor 6 (Myf6/MRF4), 432–455 and 677–657 (NM_008657); Cdk inhibitor 2B (p15Ink4b/Cdkn2b), 49–66 and 373–354 (NM_007670); Cdk4 and Cdk6 inhibitor protein (p16Ink4a), 245–264 and 653–634 (L76150); Cdk4 and Cdk6 inhibitor p18 protein (p18Ink4c), 50–70 and 462–442 (U19596); Cdk4 and Cdk6 inhibitor p19 protein (p19Ink4d), 340–360 and 732–713 (U19597); Cdk inhibitor 1A (p21Cip1/Cdkn1a), 369–391 and 691–668 (NM_007669); Cdk inhibitor 1B (p27Kip1/Cdkn1b), 87–106 and 430–410 (NM_009875); tumor suppressor p53 (p53), 930–949 and 1233–1204 (AF161020); Cdk inhibitor 1C (*p57Kip*2/Cdkn1c), 903–923 and 1242–1223 (NM_009876); *H19* and muscle-specific Nctc 1 (*H19*), 980–999 and 1344–1325 (NM_023123); insulin-like growth factor 2 (*Igf2*), 473–492 and 636–617 (M14951); reduced expression 3 (*Rex3*/*Bex1*), 326–345 and 631–612 (NM_009052); colony-stimulating factor 1 (Csf1), 557–576 and 961–942 (NM_007778); 18 S ribosomal RNA, 448–467 and 926–907 (X00686); sequence information for primers for mesoderm-specific transcript (*Peg1*/*Mest*), paternally expressed gene 1 (*Peg3*/*Pw1*); and zinc finger protein Zac1 (*Zac1*) is from a previous study (33).

RESULTS

Cardiotoxin Injection in TA Muscle Induces Extensive and Complete Regeneration—We injected cardiotoxin into the anatomically more confined TA muscles and showed regeneration in more than 90% of the myofibers (Fig. 1*A*). In three independent experiments, similar morphological changes were observed repeatedly. Histological analysis demonstrated global myofiber fragmentation and edema at days 1 and 2 after injury. The number of mononucleated cells/cross-sectional area increased significantly after cardiotoxin injection with a peak around day 3. This increase in cell number is attributable to both inflammatory cell infiltration and proliferation of satellite cells. Myotubes started to appear at day 3 and became more evident at days 5 and 10 postinjection. Morphology at day 14 postinjection was not significantly different from that of the uninjected control muscles except for the presence of central nuclei, a known hallmark of recent muscle regeneration, in nearly all myofibers. The percent BrdUrd-positive nuclei increased significantly at days 2 and 3 after injury (Fig. 1, *A* and *B*), indicating active cell proliferation. These results suggest that cardiotoxin injection in TA muscle induces extensive and complete regeneration, and the regeneration process shifts morphologically from a phase of proliferation to differentiation at around day 3 after injury.

Satellite Cell Activation and Proliferation Are Essential for Skeletal Muscle Regeneration—To assess the functional role of satellite cell activities in skeletal muscle regeneration *in vivo*, transmission electron microscopy was performed. As shown in Fig. 2*A*, satellite cell activation was apparent as early as 6 h after the cardiotoxin injection. The activated satellite cells were often separated from the adjacent myofiber, leaving electron-lucent gaps and exhibit more abundant cytoplasm and less condensed heterochromatin compared with quiescent satellite cells. At days 2 and 3 after injury, as many as seven or eight pairs of postmitotic satellite cells were often detected in a large cleft in degenerating myofiber beneath a single basal lamina. Myotubes with central nuclei and thick and thin filaments of nascent sarcomeres were apparent at day 5 postinjection. Adjacent to the myotubes were many small, mononucleated cells with condensed heterochromatin and little cytoplasm and organelles. These cells were universally in contact with both the basal lamina and the cell membrane of the growing myofiber and are likely to represent myogenic precursor cells that have reverted to a quiescent state. The timing of satellite cell activation, proliferation, and resumption of quiescence as evidenced by the morphological data is in agreement with the molecular events detected by cDNA microarray and RT-PCR observations in this study.

Inflammatory cell infiltration, as a part of the physiological responses to muscle injury, has complicated the analysis of global gene expression. A key question is how to distinguish and ascertain the contribution of myoblast proliferation from inflammatory cell infiltration. Here we performed indirect immunofluorescence for detection of BrdUrd incorporation to mark proliferative cells on control and injured (day 3) muscle sections. We also stained the same sections for MyoD, Mac-1, or ag 7/4 as markers for proliferating myoblasts (34, 35), peripheral macrophages (36), and infiltrating neutrophils (37), respectively. We predicted that a great portion of MyoD-positive cells would be positive for BrdUrd staining, and none of the Mac-1 or ag 7/4-positive cells would be positive for BrdUrd because cycling myoblasts expresses MyoD prior to terminal differentiation, whereas peripheral functional macrophages and neutrophils are terminally differentiated. Normal muscle sections showed negative results for any above mentioned staining (not shown). In any given field of a day 3 muscle section, we estimated that at least 30% of all cells were positive for MyoD, BrdUrd, or both (Fig. 2*B*). Consistent with our expectation, 45% of the MyoD-positive cells (759 cells counted) were detected positive for BrdUrd, whereas none of the cells positive for Mac-1 (508 cells counted) or ag 7/4 (114 cells counted) incorporated BrdUrd. These results provided unambiguous evidence that proliferating satellite cells are the main source of cells directly involved in myogenesis in skeletal muscle regeneration, and inflammatory cells do not proliferate in injured skeletal muscle. Those cells expressing MyoD, but with no BrdUrd incorporation, may be the cycling myoblasts in phases other than S phase of DNA replication. Our BrdUrd labeling lasted 6 h, which is only a fraction of a normal cell cycle time (~20 h) for normal mammalian cells. It is also possible that some of these MyoD-positive cells might have already exited the cell cycle and initiated the differentiation process. Consistent with this notion is the observation that many of these cells had strong staining for MyoD, which promotes myogenic differentiation (38).

To evaluate further the role of satellite cell activities in our model, gamma radiation was used to compromise the proliferative capacity of muscle stem cells, which have often been used to determine satellite cell function in skeletal muscle *in vivo* (31, 39). We subjected mouse hind limb muscles to 2,200 rads of gamma radiation 24 h before the cardiotoxin injection. Irradiated TA muscles were not morphologically different from normal TA muscles (not shown). However, myogenic cell proliferation and differentiation after cardiotoxin injection were blocked as indicated by a significantly lower increase in cell number, very few BrdUrd-positive nuclei at day 3, and the absence of newly formed myotubes at day 10 after injury (Fig. 2*C*). To confirm the findings at the molecular level, we performed semiquantitative RT-PCR to quantify transcripts for Cdc6, myogenin, and p57Kip2; their expression has been shown previously to be essential for cell proliferation or myogenesis (18, 40, 41). Irradiated TA muscles had attenuated or delayed induction of these transcripts (Fig. 2*D*), suggesting that satellite cells play a pivotal role in skeletal muscle regeneration.

Comprehensive Microarray Analysis Defines Phasic Changes in Gene Expression and Identify Novel Genes Regulated during Muscle Regeneration—To investigate global gene expression during injury-induced skeletal muscle regeneration, cDNA microarray hybridizations were performed using a National Institute on Aging mouse 16,000-byte cDNA chip. Of 16,267 elements screened, 3,532 (21.7%) were altered more than 2.5-fold at one or more time points. A significant number of genes were altered during the early phase of regeneration before day 5 after cardiotoxin injection as shown by the scatter plots (Fig. 3*A*). The trend became less evident as regeneration approached completion by days 10 and 14 after injury. Quantification confirmed a phasic change in the number of differentially expressed genes (>2.5-fold change) with a peak around day 2 (2,310 elements, 14.2% of total) and day 3 (2,324 elements, 14.3% of total) after injury (Fig. 3*B*). By day 14 after cardiotoxin injection, only 199 gene elements (1.2% of total) showed differential expression.

The self-organizing map (32) was used to assemble and analyze the data. The clustering procedure groups together cDNA elements on the basis of their common expression patterns over the time points. 16 cluster groups were used (Fig. 3*C*). Fig. 4 shows part of the results of a hierarchical clustering as described previously (42), and complete results are presented as supplemental data (self-organization map in supplemental data 1 and functional groups in supplemental data 2) in the *Journal of Biological Chemistry* on-line. In most cases, redun-

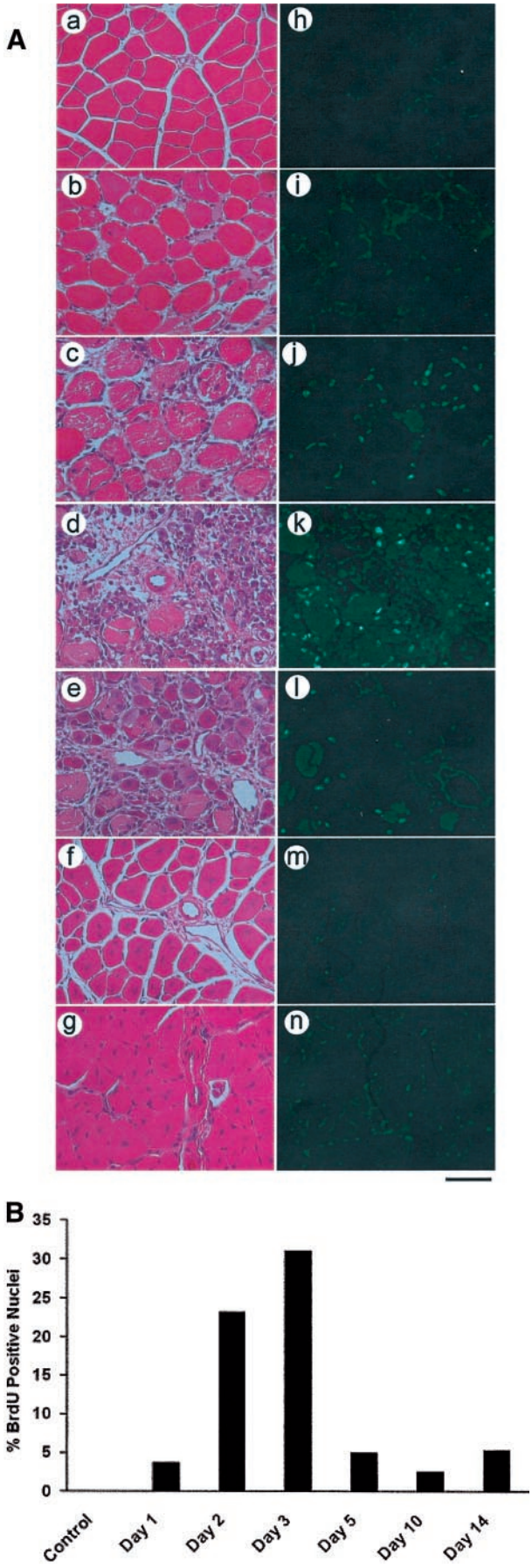

FIG. 1. **Cardiotoxin injection-induced muscle regeneration in TA muscle.** *A*, serial sections from control (*a* and *h*) and injured TA muscles at day 1 (*b* and *i*), day 2 (*c* and *j*), day 3 (*d* and *k*), day 5 (*e* and *l*), day 10 (*f* and *m*), and day 14 (*g* and *n*) postinjection were stained with H&E (*a–g*) or anti-BrdUrd antibodies (*h–n*). The *scale bar* equals 100 μm. *B*, quantification of BrdUrd-positive nuclei in control and TA muscles at various times after cardiotoxin injection. Data are presented as the means from two measurements, each with more than 100 in randomly selected areas in cross-sections.

dant cDNA probe sets were in the same cluster or in clusters with similar profiles. For example, eight redundant H2A histone family member Z gene elements were clustered in c5, and seven mouse heat shock protein 86 were clustered in c4 and c8 with a similar expression pattern. These results confirmed the fidelity of the microarray analysis used in this study. Furthermore, many functionally related genes were clustered together. For example, 48 gene elements related to energy and metabolism were clustered in c14 (26.8%, total 179 elements). There is a nearly 4-fold enrichment of these gene elements in this cluster because there are 258 gene elements related to energy and metabolism in the population (7.3%, total 3,532 elements). These findings indicate that the assay system is suitable for detecting genetic regulatory events during muscle regeneration, and we could use the hierarchical cluster analysis to identify novel genes with expression patterns similar to those well known functional genes.

To identify novel genes related to myogenic differentiation, we focused our attention on genes with a peak expression pattern concurrent with muscle differentiation. For example, we noticed that three paternally imprinted genes, *H19*, *p57Kip2*, and *Rex3*/*Bex1*, and four maternally imprinted genes, *Igf2*, *Peg1*/*Mest*, *Peg3*/*Pw1*, and *Zac1*, are clustered in c3 and/or c1. Because genes in these two clusters have peak induction of mRNA at day 3 or day 5, concurrent with morphological signs of myogenic differentiation, coordinated induction of these genes may play important functional roles in muscle differentiation. We also noticed similar induction of bone morphogenetic protein-6, growth arrest-specific 7 (Gas-7) and Gas-1 transcripts in c1, all of which encode antagonists to sonic hedgehog (Shh) signaling pathways. This points to the possible roles of these antagonists in myogenic differentiation.

Induction of E2f and Cell Cycle Gene Transcripts Marks the Proliferative Phase of Skeletal Muscle Regeneration—A total of 36 transcripts encoding regulators of cell cycle progression and DNA replication were clustered in c4 (14 elements), c5 (11 elements), and c8 (11 elements) clusters. One common feature of the expression profiles of these clusters is their early induction and peak expression at day 2 or day 3 and declined expression after day 3 following injury. This is in strong agreement with the morphological finding that active cell proliferation occurs during the early phase of regeneration. To confirm the microarray results and obtain comprehensive information for genes with functions in the proliferation program, we performed semiquantitative RT-PCR for transcripts of DNA replication factors, cyclins, and Rb/E2f/DP transcription factors. DNA replication factors (Cdc6, Mcmd2, Mcmd3, Orc1 and Orc2) and cyclins (cyclin A2, cyclin B, cyclin D1, cyclin D2, cyclin D3, cyclin E, and cyclin E2) all had an early induction in mRNA abundance at day 1, peaking around day 2 or day 3, and started to return to the control level after day 3 following injury (Fig. 5, *A* and *B*). Because many of these genes are regulated by Rb/E2f/DP transcription factors (6, 43), it is desirable to determine which of the Rb/E2f/DP transcription factors may participate during skeletal muscle regeneration *in vivo*. Therefore, we measured Rb (Rb, p107, and p130), E2f (E2f1, E2f2, E2f3, E2f4, E2f5, and E2f6) and DP (DP-1 and DP-3) transcripts by semiquantitative RT-PCR (Fig. 5*C*). Consistent with the microarray data, we observed an initial reduction of E2f6 after injury and minimal increases in E2f3, E2f4,

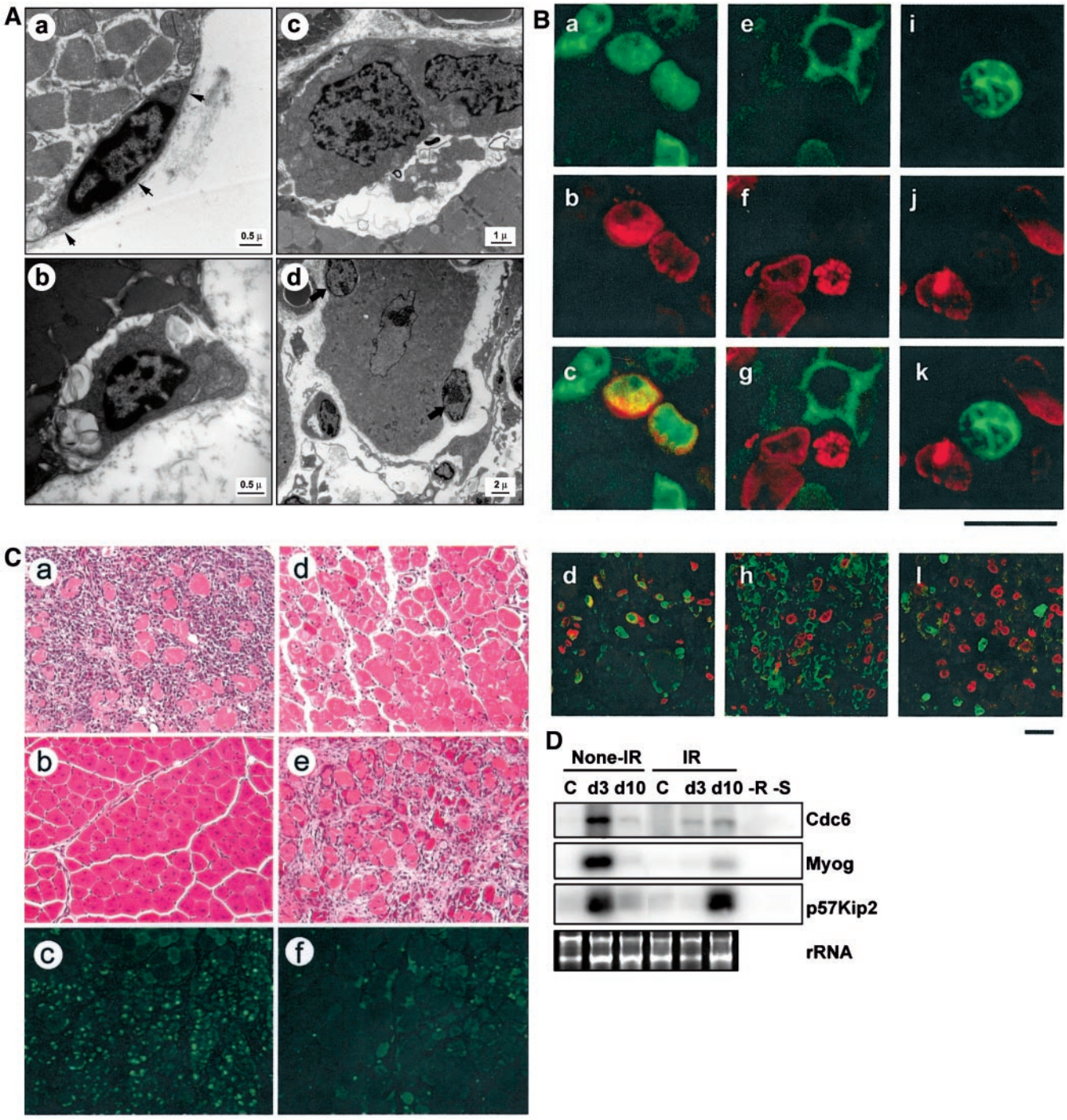

FIG. 2. **Satellite cell activities in adult skeletal muscle regeneration.** *A*, satellite cell activity assessed by transmission electron microscopy. *a*, a quiescent satellite cell in a control TA muscle, showing characteristically condensed heterochromatin in the nucleus and little cytoplasmic fraction. The cell lies in close contact between the mature myofiber and the continuous basal lamina (indicated by *arrows*). *b*, an activated satellite cell with pseudopodia, less condensed heterochromatin, and increased cytoplasmic fraction near a degenerating myofiber 6 h after cardiotoxin injection. There are noticeable spaces between the activated satellite cell and the degenerating myofiber. *c*, two newly divided progeny cells after cell division in a regenerating myofiber at day 2 after injury. The heterochromatin in these cells is significantly less dense. *d*, a myotube with a central nucleus and two satellite cells (indicated by *arrows*) at day 5 after cardiotoxin injection. *B*, assessment of satellite cell, macrophage, and neutrophil in cell proliferation during skeletal muscle regeneration. Muscle sections were stained for MyoD (*a*), Mac-1 (*e*), or ag 7/4 (*i*) with primary antibodies and fluorescein isothiocyanate-conjugated secondary antibody (*green colored* images) with a simultaneous staining for BrdUrd on the same sections (*b*, *f*, and *j*, respectively) with anti-BrdUrd primary antibody followed by rhodamine-conjugated secondary antibody (*red colored* images). The merged images are presented at high magnification (*c*, *g*, and *k*) and low magnification (*d*, *h*, *l*) below the *single colored* images. Cells positive both for BrdUrd and MyoD are shown in *yellow*. *Scale bars* equal 20 μm. C, compromised cell proliferation in the absence of active satellite cells. *a*, H&E staining of injured TA muscle at day 3 after the cardiotoxin injection. There is a significant accumulation of mononucleated cells in the injured area. *b*, H&E staining of injured TA muscle at day 10 after the cardiotoxin injection. Newly formed myotubes with central nuclei are present uniformly. *c*, immunofluorescence staining with anti-BrdUrd antibody of injured TA muscle at day 3 after the cardiotoxin injection, showing active DNA replication as indicated by positive BrdUrd staining. *d*, H&E staining of injured irradiated TA muscle at day 3 after the cardiotoxin injection. Compared with injured TA muscle without prior irradiation at the same time point, there is significantly less accumulation of mononucleated cells. *b*, H&E staining of injured irradiated TA muscle at day 10 after the cardiotoxin injection showing the presence of degenerative muscle debris and mononucleated cells with no indication of myotube formation. *c*, immunofluorescence staining with anti-BrdUrd antibody of injured irradiated TA muscle at day 3 after the cardiotoxin injection. There are few BrdUrd-positive cells. *D*, blocked/

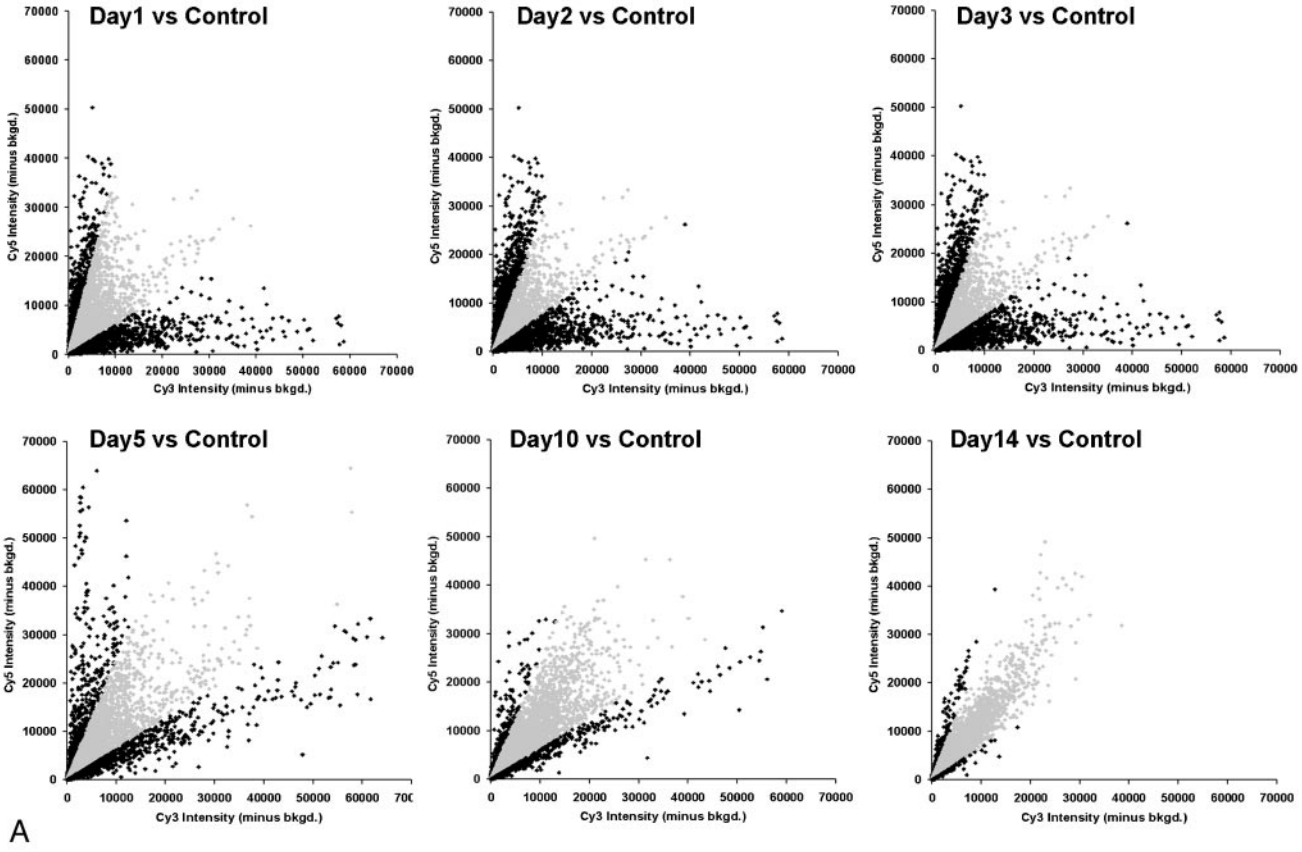

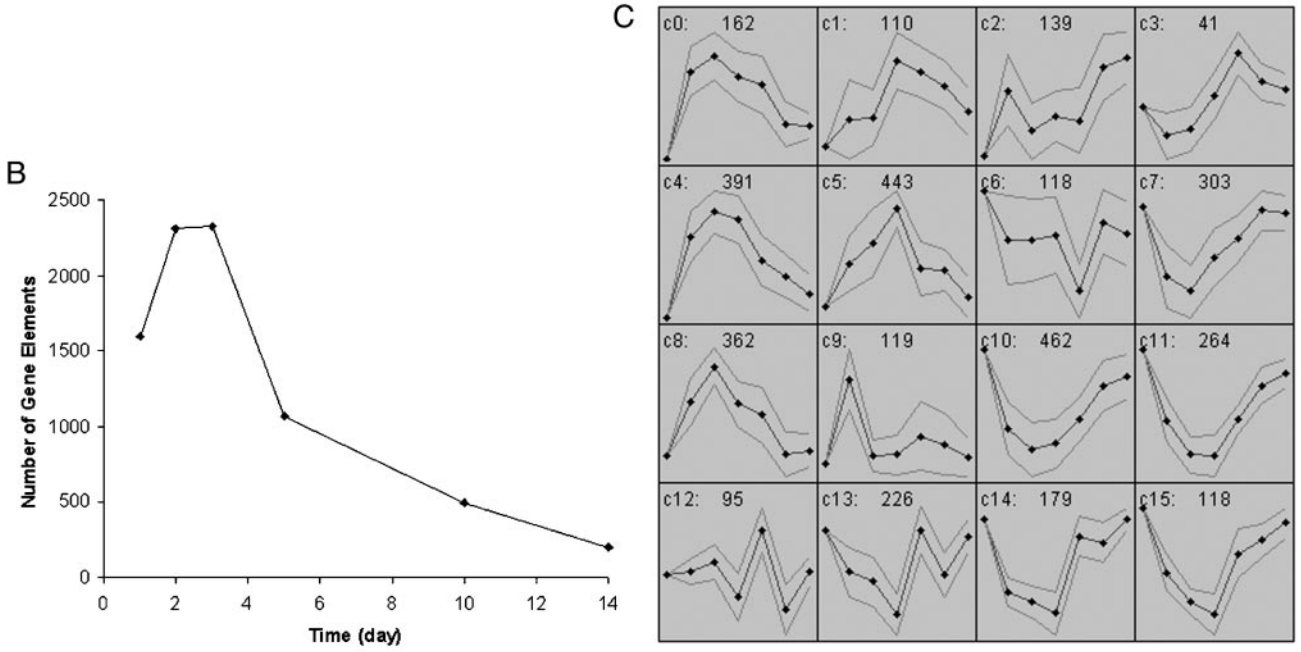

FIG. 3. **Microarray analysis of global gene expression during skeletal muscle regeneration.** *A*, scatter plots for comparison between control (Cy3 signals) and injured (Cy5 signals) TA muscles for 16,267 gene elements at days 1, 2, 3, 5, 10, or 14 after the cardiotoxin injection. Each individual *dot* in a plot represents a data point from a single gene element. *Gray dots* indicate that the difference between the control and injured muscles is ≤2.5-fold. *Solid dots* indicate that the difference between the control and injured muscles is >2.5-fold. *B*, quantification of the number of gene elements that showed >2.5-fold change at various time points. *C*, self-organization map clusters using the 3,532 regulated expression profiles. The number of clusters was specified as 16, and an algorithm grouped them into discrete clusters. *c0–c15* indicates the cluster number, and the *number* in the *top middle* of each *box* indicates the number of gene elements in each cluster. Time points are 0, 1, 2, 3, 5, 10, and 14 days, designated by *black dots* from *left* to *right*, where the 0 time point is the assumed log2 ratio of 0 between control samples. *Thick lines* represent the mean expression values, and *thin lines* represent the standard deviations.

delayed activation of marker genes for cell proliferation and differentiation in irradiated TA muscle. Semiquantitative RT-PCR was performed for uninjected control (*C*), at day 3 (*d3*) or at day 10 (*d10*) after cardiotoxin in nonirradiated (*none-IR*) or irradiated (*IR*) TA muscles. Reactions without total RNA sample (−*S*) or without reverse transcriptase (−*R*) were used as negative controls.

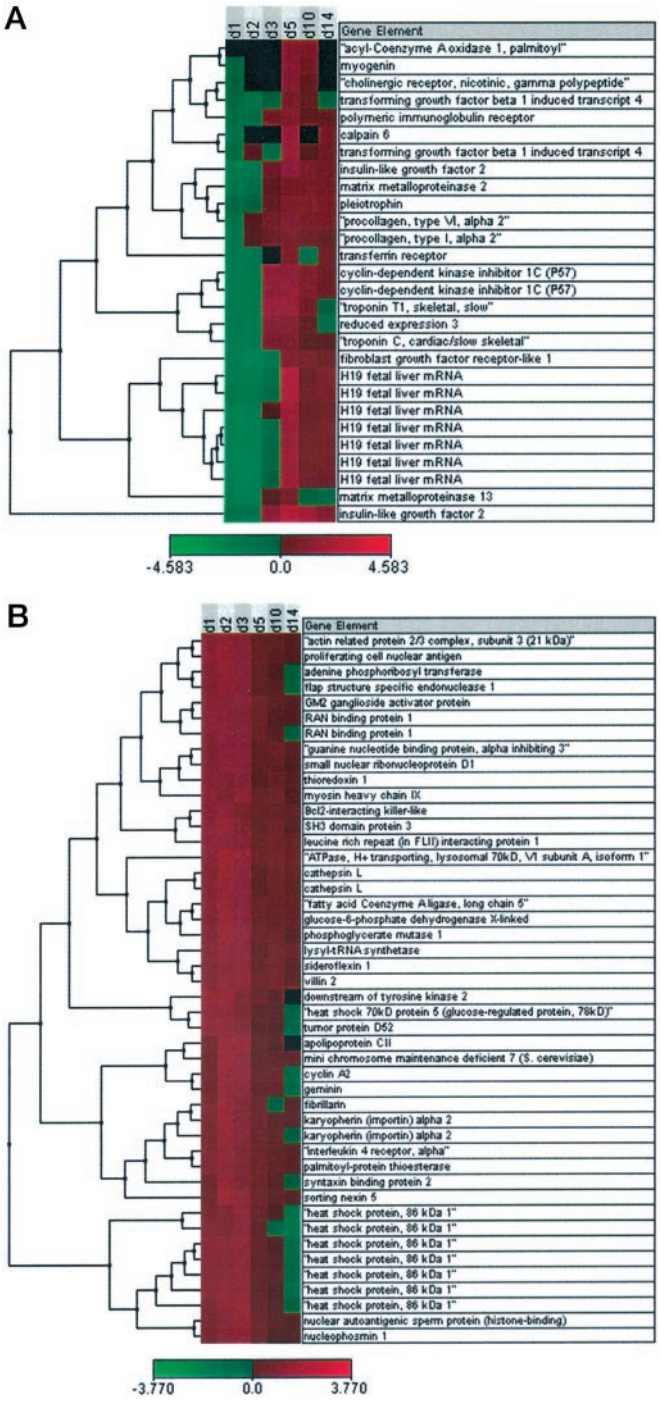

FIG. 4. **Hierarchical clustering analysis of expression profiles.** *A*, the genes with distinct transient induction grouped by self-organizing map in c3 are clustered by correlation of the profiles. Gene names are plotted along the *x* axis, with each block representing a time point. Increases or decreases in mRNA levels are represented as shades of *red* and *green*, respectively. *B*, part of the genes grouped in c4. The figures are generated by J-Express (MolMine AS, Bergen, Norway; www.molmine.com).

and E2f5 transcripts, whereas E2f1 and E2f2 were highly induced during the proliferative phase of muscle regeneration between days 1 and 3 after injury. DP-1 was transiently induced, and DP-3 had a minimal change during regeneration. Members in the Rb family have distinct expression patterns from each other. Induction of p107 was concurrent with that of E2f1, E2f2, and DNA replication factors. Induction of Rb transcript is not obvious until day 3 after injury, in agreement with its role in induction of muscle differentiation, whereas p130 remained almost the same during the entire regeneration process. The concurrent induction of genes essential for DNA replication and cell cycle control with significant induction of E2f1, E2f2, p107, and DP-1 transcripts promoted us to postulate that these regulatory proteins are essential for satellite cell proliferation *in vivo* during muscle regeneration.

Coordinated Expression of Myogenic Factors and Cyclin-dependent Kinase Inhibitors Defines a Transition from Cell Proliferation to Differentiation—Transcripts in c3 and c1 showed no induction until day 3 and day 5 after injury, respectively (Fig. 3*C*). Peak expression of these genes corresponds to muscle differentiation/maturation defined by morphological analyses. Many muscle-specific genes or genes that are known to be induced during skeletal muscle differentiation were grouped in these clusters. For example, cardiac and slow twitch skeletal muscle Ca^{2+}-ATPase (*Atp2a2*), slow twitch skeletal muscle troponin T (*Tnnt1*), *Igf2*, nicotinic cholinergic receptor α polypeptide 1 (*Chrna1*), fibroblast growth factor receptor 4 (*Fgfr4*), *Peg1/Mest*, *p57Kip2*, cardiac troponin T2 (*Tnnt2*), *H19*, transforming growth factor β1-induced transcript 4 (*Tgfb1i4*), nicotinic cholinergic receptor γ polypeptide (*Chrng*), *Igf1*, myogenin and cardiac and slow-twitch skeletal muscle troponin C (*Tncc*) were grouped in these two clusters. It is important to notice that a majority of these transcripts did not show a significant increase in irradiated muscles 3 days after cardiotoxin injection, suggesting that up-regulation of these genes depends on the presence of satellite cell activities. Induction of these genes defines, at the molecular level, myogenic differentiation that occurs around day 3 in our regeneration model.

To confirm the microarray findings and obtain comprehensive information of myogenic transcription factors and cell cycle inhibitors, we performed semiquantitative RT-PCR and revealed distinct expression profiles for different myogenic transcription factors and Cdk inhibitors in adult muscle regeneration (Fig. 5, *D* and *E*). First, compared with the uninjected control TA muscle, Pax3 and MRF4 expression showed minimal changes during muscle regeneration. Second, there was an early induction of MyoD with a peak expression at day 3, preceding that of Myf5 at day 5 after injury. Third, a sharp induction was observed for Pax7 and myogenin at day 3 after injury concurrent with myogenic differentiation. For the Cdk inhibitors, microarray analysis showed that the p18Ink4c transcript was transiently induced during the proliferative phase of muscle regeneration (in c5), whereas the $p57^{kip2}$ transcript was induced during muscle differentiation (in c1 and c3). RT-PCR analysis confirmed these findings (Fig. 5*E*). Remarkably, a highly coordinated peak induction of transcripts for three other Cdk inhibitors occurred at day 3 after injury, which includes p16Ink6a, p15Ink4b and p21Cip1, whereas p19Ink4d and p27Kip1 showed less dramatic changes during the repair process.

Comparison between Normal and Irradiated Muscle Is Useful in Assessing Satellite Cell Contribution to Changes in Global Gene Expression—One of the major limitations of analysis of global gene expression for an *in vivo* study is the heterogeneity of the composition of the tissue samples. It is difficult to ascertain which cell population is responsible for the changes detected in the expression profile. More specifically, we do know not whether induced or reduced expression of a gene of interest is a direct result of satellite cell proliferation and differentiation or of inflammatory cell infiltration. It is certainly not practical to determine cell-specific expression for all of the genes surveyed in the microarray hybridization using any of the exiting morphological analyses. We decided to take advantage of gamma radiation to eliminate satellite cell activities in adult skeletal muscle. As we have shown in this study,

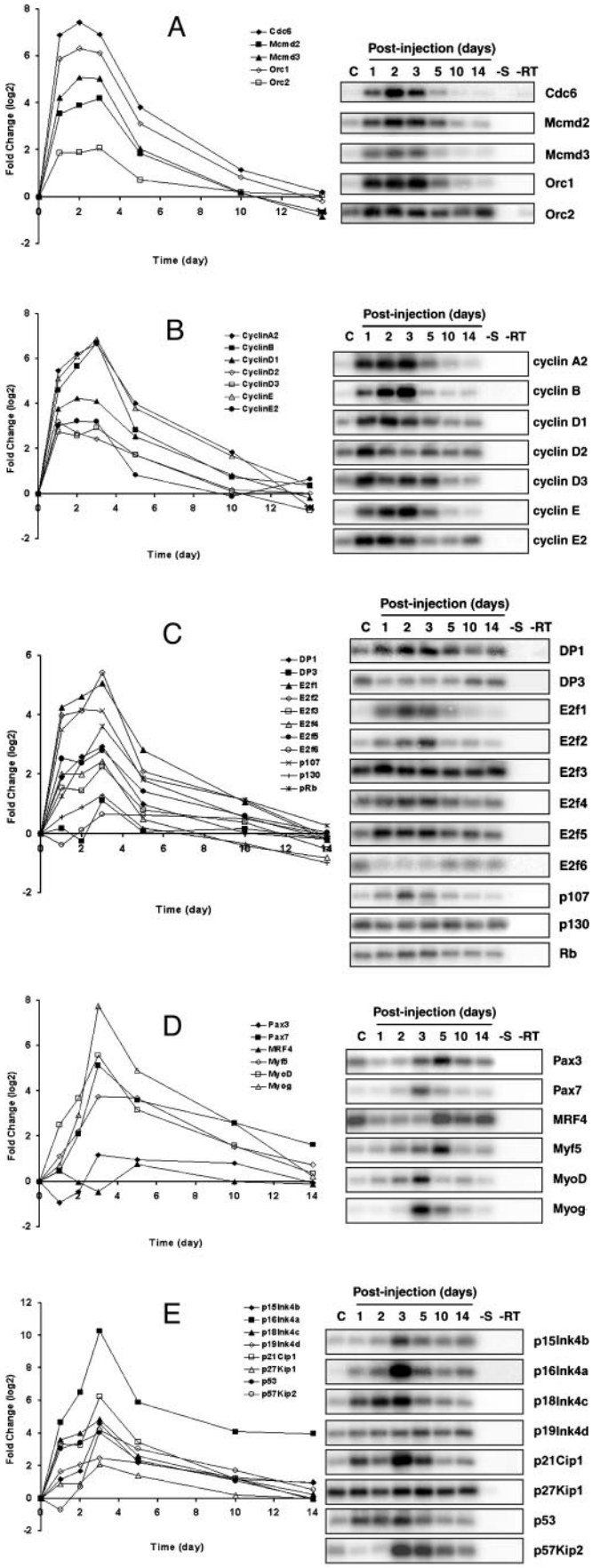

FIG. 5. **RT-PCR analysis of expression profiles for genes related to cell cycle and DNA replication control and muscle differentiation.** Semiquantitative RT-PCR was performed for genes encoding proteins for DNA replication (*A*), cyclins (*B*), Rb/E2f/DP transcription factors (*C*), myogenic regulatory factors (*D*), and cyclin-dependent kinase inhibitors (*E*) as described previously (22). Representative images are presented for each specific gene element after Southern blot hybridization of the PCR products with ^{32}P-labeled random primers. Quantitative data ($n = 3$) are presented on the *left* of each *graph*. Reactions without total RNA sample ($-S$) or without reverse transcriptase ($-R$) were used as negative controls.

gamma radiation of hind limb muscles at 24 h prior to muscle injury can successfully eliminate satellite cell activities, blocking myogenic cell proliferation and differentiation. We assessed the global gene expression in irradiated muscles without cardiotoxin injection, which provides information regarding the effects of gamma radiation alone, and in irradiated muscles at day 3 after cardiotoxin injection, which provides background information regarding altered gene expression in the absence of satellite cell activity. Among 3,532 elements that were shown to have more than a 2.5-fold change during the time course, 211 and 1,772 gene elements showed more than 2.5-fold change in the irradiated muscles without and with injury, respectively (see supplemental data).

To determine whether this approach is useful in assessing satellite cell contribution to changes in global gene expression, we used RT-PCR analysis to compare gene expression between normal and irradiated samples (Fig. 6). Induction of Csf1 mRNA, a marker for macrophages, was not affected by irradiation, suggesting that inflammatory cell infiltration was not affected by irradiation. In addition to the gene elements that had been tested (Cdc6, myogenin, and p57Kip2, Fig. 2*D*), we analyzed nine genes (cyclin A2, cyclin B, cyclin D1, p107, Mcmd2, Mcmd3, MyoD, E2f1, and E2f2) that are related to cell cycle or myogenesis and had been confirmed to be induced during regeneration. Induction of all these genes, except for cyclin D1, was abolished in the irradiated muscles at day 3 after injury. The RT-PCR data are in complete agreement with the microarray data. The finding on cyclin D1 is not surprising because a recent study also showed persistent stretch-induced induction of cyclin D1 in irradiated muscles, suggesting that cyclin D1 plays additional role other than myogenesis *in vivo*. Cluster analysis grouped a subset of imprinted genes with well known myogenic regulatory factors, such as myogenin. We postulated that coordinated expression of these imprinted genes is of importance to myogenic differentiation. To test this hypothesis, we performed the same analysis for all seven imprinted genes (*H19*, *Zac1*, *Igf2*, *p57kip2*, *Peg1*, *Peg3*, *Rex3*) that had profiles similar to those genes encoding myogenic factors, such as myogenin. Induction of all these imprinted genes, except for *H19*, were abolished in irradiated muscles after injury. The reason for not detecting *H19* mRNA induction may be that we did not use the time point (day 5) when *H19* was shown to be significantly induced. Overall, these results further support our hypothesis that coordinated induction of these imprinted genes may play pivotal roles in muscle differentiation *in vivo*. Therefore, we believe cardiotoxin injection in irradiated muscle provides valuable background information for assessment of the contribution of satellite cell activities in global gene expression in this regeneration model. For this reason, we chose to present the microarray data from the irradiated muscles along with the time course data.

Targeted Mutation of E2f1, but Not of E2f2, Compromises Skeletal Muscle Regeneration—Because both E2f1 and E2f2 are highly induced during skeletal muscle regeneration concurrent with many genes related to the control of the cell cycle and DNA replication, we speculated that they both participated in regeneration by regulating those genes transcriptionally. To determine whether E2f1 or E2f2 is required for adult skeletal

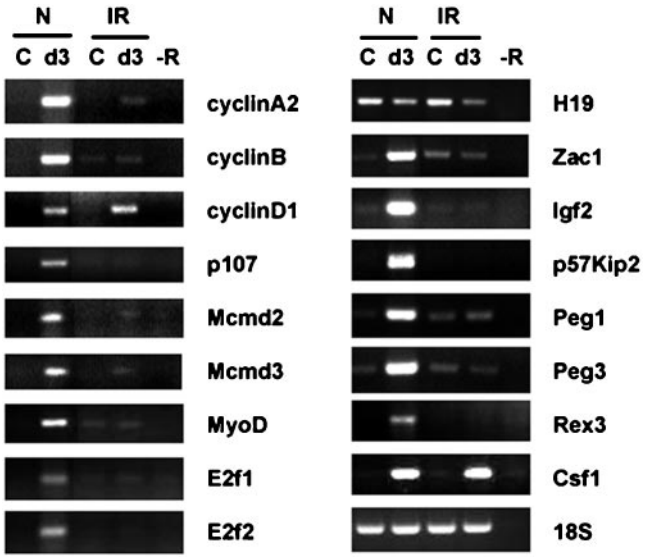

FIG. 6. **RT-PCR analysis for a direct comparison between normal and irradiated muscles before and after cardiotoxin injection.** Semiquantitative RT-PCR was performed for imprinted genes and genes related to cell cycle control and myogenic differentiation. Representative images are presented for each specific gene element after resolving the PCR products on 1.5% agarose gel and staining with ethidium bromide. Similar results were obtained from three independent sample sets. Reactions without reverse transcriptase (*−R*) were used as negative controls.

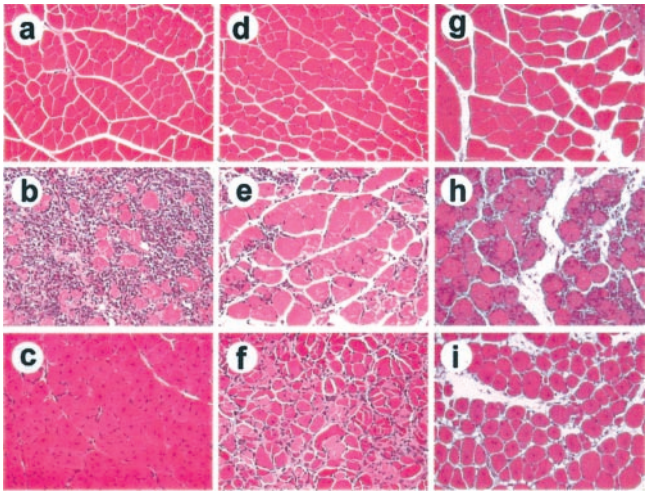

FIG. 7. **E2f1$^{-/-}$ mice are defect in muscle regeneration.** H&E staining of TA muscles of wild-type (*a–c*), E2f1$^{-/-}$ (*d–f*), and E2f2$^{-/-}$ (*g–i*) mice without injury (*a*, *d*, and *g*), at day 3 after injury (*b*, *e*, and *h*), and at day 10 after injury (*c*, *f*, and *i*). There is no significant morphological difference in the uninjured TA muscle cross-sections among the wild-type, E2f1$^{-/-}$, and E2f2$^{-/-}$ mice. Both the E2f1$^{-/-}$ and E2f2$^{-/-}$ muscles have less mononucleated cell accumulation at day 3 after the cardiotoxin injection. At day 10 after injury, only E2f1$^{-/-}$ TA muscle shows little sign of nascent myotube formation and the noticeable presence of mononucleated cells.

muscle regeneration, we performed cardiotoxin injection in TA muscles in mice with targeted mutation of E2f1 or E2f2. As shown in Fig. 7, mice with targeted mutation of E2f2 had a relatively normal regeneration process compared with wild-type mice, whereas muscle regeneration was severely compromised in mice with targeted mutation of E2f1. Therefore, we have confirmed that E2f1, but not E2f2, is essential for muscle regeneration *in vivo*.

DISCUSSION

Injury-induced regeneration in mouse skeletal muscle is a useful model to study satellite cell function *in vivo* (21, 22, 44). Here, we modified a previously described animal model (22, 45) and showed extensive and complete regeneration *in vivo* as assessed by morphology, DNA replication, and mRNA expression profiles. Microarray and semiquantitative RT-PCR analyses and comparison between normal and irradiated muscles in this regeneration model define new insights into molecular events important for control of proliferation and differentiation in satellite cells *in vivo*.

The ability to assay and analyze a very large number of genes with respect to mRNA expression using microarray analysis provides an opportunity to reveal unsuspected functions of known and novel genes. This technology has recently been used successfully to study gene regulation in skeletal muscle (46–52). In this study, we were able to map seven imprinted genes (*Bex1*, *H19*, *p57Kip2*, *Igf2*, *Peg1/Mest*, *Peg3/Pw1*, and *Zac1*) into two transcript clusters with profiles indicative of importance for muscle differentiation. Four of these genes, *H19*, *p57Kip2*, *Peg3/Pw1*, and *Igf2*, have previously been shown to be regulated during skeletal muscle development (41, 53–55). We confirmed that the induction of six of these imprinted genes by muscle injury was abolished in the irradiated muscles, further supporting the notion that they play important role in satellite cell activities during muscle regeneration because gamma radiation eliminates satellite cell proliferation and blocks muscle regeneration. One intriguing question related to these findings is how these imprinted genes are regulated during the regeneration process. The simplistic explanation is that muscle injury enhances monolellic expression of these genes as a result of increased transcriptional activity. It is also formally possible that there is an epigenetic reprogramming because epigenetic modification to DNA or chromatin plays a role in determining gene activity (56). In another word, these genes begin to express from the imprinted allele in the injured muscle. Nevertheless, a highly coordinated expression of imprinted genes in muscle regeneration *in vivo* has been first noticed in this study. A comprehensive analysis of expression of imprinted genes in this model is likely to yield new information regarding the importance of epigenetic regulation during muscle regeneration.

A transient induction of bone morphogenetic protein-6, Gas-7, and Gas-1 transcripts contemporaneous with myogenic differentiation suggests the importance of these antagonists to the Shh signal transductions in muscle differentiation. The Shh signaling pathway is important for the activation of myogenesis in mammals (57, 58), and Shh signaling is required for maintenance of Myf5 and MyoD and for the correct timing of terminal differentiation in zebrafish development (59). Our study identifies potential antagonist signaling molecules in these pathways pertinent to muscle differentiation *in vivo*.

We employed gamma radiation to cause reproductive death of satellite cells, which showed no discernible effect on morphology of uninjured muscle. However, this treatment blocked DNA replication and myotube formation and blocked/delayed induction of Cdc6, myogenin, and p57Kip2 transcripts, indicating that satellite cell activation and proliferation are abolished by gamma radiation. Therefore, cardiotoxin injection in irradiated muscles could provide valuable background information for assessment of the contribution of satellite cell activities in global gene expression during skeletal muscle regeneration.

The functional relationship among myogenic transcription factors in governing myogenic differentiation has been defined by studies in developing mouse embryos (21, 23–30). Our observation that an early induction of MyoD transcript during the proliferative phase of muscle regeneration precedes a sharp induction of MyoG at differentiation is consistent with a role for

a MyoD-myogenin cascade in myogenic differentiation. The expression pattern of MyoD transcripts detected in this study is also consistent with its multiple functions in myogenic cell maintenance and differentiation. A unique finding in this study is the induction of Myf5. Peak expression of Myf5 was not induced until after the induction of Pax7 and myogenin and initiation of differentiation, implying that the function of Myf5 and/or its regulation are fundamentally different between embryonic development of skeletal muscle and adult muscle regeneration. The evidence supporting this hypothesis is the previous finding that targeted mutation of MyoD leads to normal skeletal muscle development in association with compensatory expression of Myf5 (17), but adult skeletal muscles lacking MyoD gene are defective in muscle regeneration (44, 60). Because Pax7 is required for the satellite cell lineage specification and Myf5 is expressed in quiescent satellite cells (61, 62), we hypothesize that the Pax7-Myf5 cascade plays a cooperative role in specifying and renewing the satellite cell pool during skeletal muscle regeneration *in vivo*. Collectively, results from this study suggest that the transcription factors governing myogenic differentiation play distinct roles during adult muscle regeneration from that observed during myogenesis in embryonic development.

What mechanisms are responsible for coupling cell cycle withdrawal with muscle differentiation? Proteins that are capable of inhibiting the cell cycle and promoting myogenesis may serve such a function. In the present study, we quantified mRNA expression of all known Cdk inhibitors during muscle regeneration *in vivo*. We observed highly coordinated induction of several transcripts for Cdk inhibitors at the time of myogenic differentiation, among which p15Ink4b, p18Ink4c and p16Ink4a are specific inhibitors for Cdk4 and Cdk6 and p21Cip1, and p57Kip2 are broader Cdk inhibitors. Remarkably, p57Kip2 and p21Cip1 are known to be essential for myogenesis acting on myogenin (41), and p57Kip2 stabilizes MyoD by a direct interaction (63) and by inhibition of cyclin E/Cdk2 (64). Similarly, both p16Ink4a and p18Ink4c have also been implicated in promoting myogenic differentiation independent of their inhibition of Cdk4 and Cdk6 (65–67). Hence, highly coordinated induction of Cdk inhibitors may inhibit cell cycle progression and trigger cell cycle exit, whereas promoting myogenesis coordinating regulatory cross-talk between the proliferation and differentiation genetic programs *in vivo*.

Satellite cell reentry into the cell cycle from quiescence requires activation of the Cdk/Rb/E2f signaling pathway. The regulatory step that involves E2f transcription factors is critical in this process because E2f regulates genes involved in DNA replication and cell cycle progression (7, 14, 68–70). In this study, we observed transient induction of Cdc6, Orc1, Orc2, Mcmd2 and Mcmd3 transcripts as well as most of the cyclins with a pattern similar to transcription factors DP1, p107, E2f1, and E2f2. This unique combinatory induction of Rb/E2f genes commits myogenic stem cells in cell cycle during regeneration *in vivo*. We are beginning to determine the functional role of some of these individual members in the control of cell proliferation during muscle regeneration. We wondered whether both E2f1 and E2f2 are required for muscle injury-induced satellite proliferation and regeneration. Injection of cardiotoxin in TA muscles of mice with targeted mutation of E2f1 results in severely compromised muscle regeneration as indicated by the persistent presence of degenerative debris and fewer and less mature myotubes at the late phase of muscle regeneration. Whether the absence of induction of E2f1 leads to defects in apoptosis, which in turn leads to defective muscle regeneration, remains to be ascertained because it has been reported recently that E2f1 induces apoptosis through a p53-dependent pathway in mammalian cells (71). The relatively normal regeneration process in E2f2 null mice is unexpected, but it suggests that disruption of E2f2 expression alone is not sufficient to cause retardation of muscle regeneration. Although this study does not rule out the possibility that the other E2f transcription factors play fundamentally important roles through different regulatory mechanisms such as protein phosphorylation and/or degradation, the results presented here provide direct evidence that E2f1 and E2f2 play distinct roles in adult skeletal muscle regeneration.

Acknowledgments—We thank E. N. Olson, R. Bassel-Duby, and B. Annex for comments; J. R. Nevins for providing E2f2 null mice; and A. Pippen, R. E. Rempel, J. M. Shelton, S. C. Williams, C. Pomajzl, and J. M. Stark for excellent technical support.

REFERENCES

1. Pearce, G. W., and Walton, J. N. (1962) *J. Neurol. Bacteriol.* **83,** 535–550
2. Pearson, C. M. (1962) *Brain* **85,** 109–118
3. Bischoff, R. (1994) in *Myogenesis* (Franszini-Armstrong, A. G. E. a. C., eds) pp. 97–118, McGraw-Hill, Inc., New York
4. Grounds, M. D., and Yablonka-Reuveni, Z. (1993) *Mol. Cell. Biol. Hum. Dis. Ser.* **3,** 210–256
5. Anderson, J. E. (1998) *Biochem. Cell Biol.* **76,** 13–26
6. Nevins, J. R. (1998) *Cell Growth Differ.* **9,** 585–593
7. Dyson, N. (1998) *Genes Dev.* **12,** 2245–2262
8. Won, K. A., Xiong, Y., Beach, D., and Gilman, M. Z. (1992) *Proc. Natl. Acad. Sci. U. S. A.* **89,** 9910–9914
9. Cheng, M., Sexl, V., Sherr, C. J., and Roussel, M. F. (1998) *Proc. Natl. Acad. Sci. U. S. A.* **95,** 1091–1096
10. Kato, J., Matsushime, H., Hiebert, S. W., Ewen, M. E., and Sherr, C. J. (1993) *Genes Dev.* **7,** 331–342
11. Ewen, M. E., Sluss, H. K., Sherr, C. J., Matsushime, H., Kato, J., and Livingston, D. M. (1993) *Cell* **73,** 487–497
12. Sears, R., Ohtani, K., and Nevins, J. R. (1997) *Mol. Cell. Biol.* **17,** 5227–5235
13. Galaktionov, K., Chen, X., and Beach, D. (1996) *Nature* **382,** 511–517
14. Leone, G., DeGregori, J., Yan, Z., Jakoi, L., Ishida, S., Williams, R. S., and Nevins, J. R. (1998) *Genes Dev.* **12,** 2120–2130
15. Olson, E. N., Brennan, T. J., Chakraborty, T., Cheng, T. C., Cserjesi, P., Edmondson, D., James, G., and Li, L. (1991) *Mol. Cell. Biochem.* **104,** 7–13
16. Braun, T., Rudnicki, M. A., Arnold, H. H., and Jaenisch, R. (1992) *Cell* **71,** 369–382
17. Rudnicki, M. A., Braun, T., Hinuma, S., and Jaenisch, R. (1992) *Cell* **71,** 383–390
18. Hasty, P., Bradley, A., Morris, J. H., Edmondson, D. G., Venuti, J. M., Olson, E. N., and Klein, W. H. (1993) *Nature* **364,** 501–506
19. Zhang, W., Behringer, R. R., and Olson, E. N. (1995) *Genes Dev.* **9,** 1388–1399
20. Lin, Q., Lu, J., Yanagisawa, H., Webb, R., Lyons, G. E., Richardson, J. A., and Olson, E. N. (1998) *Development* **125,** 4565–4574
21. Seale, P., Sabourin, L. A., Girgis-Gabardo, A., Mansouri, A., Gruss, P., and Rudnicki, M. A. (2000) *Cell* **102,** 777–786
22. Garry, D. J., Meeson, A., Elterman, J., Zhao, Y., Yang, P., Bassel-Duby, R., and Williams, R. S. (2000) *Proc. Natl. Acad. Sci. U. S. A.* **97,** 5416–5421
23. Williams, B. A., and Ordahl, C. P. (1994) *Development* **120,** 785–796
24. Ridgeway, A. G., and Skerjanc, I. S. (2001) *J. Biol. Chem.* **276,** 19033–19039
25. Davis, R. L., Weintraub, H., and Lassar, A. B. (1987) *Cell* **51,** 987–1000
26. Braun, T., Buschhausen-Denker, G., Bober, E., Tannich, E., and Arnold, H. H. (1989) *EMBO J.* **8,** 701–709
27. Edmondson, D. G., and Olson, E. N. (1990) *Genes Dev.* **4,** 1450
28. Rhodes, S. J., and Konieczny, S. F. (1989) *Genes Dev.* **3,** 2050–2061
29. Cserjesi, P., and Olson, E. N. (1991) *Mol. Cell. Biol.* **11,** 4854–4862
30. Molkentin, J. D., Black, B. L., Martin, J. F., and Olson, E. N. (1995) *Cell* **83,** 1125–1136
31. Phelan, J. N., and Gonyea, W. J. (1997) *Anat. Rec.* **247,** 179–188
32. Tamayo, P., Slonim, D., Mesirov, J., Zhu, Q., Kitareewan, S., Dmitrovsky, E., Lander, E. S., and Golub, T. R. (1999) *Proc. Natl. Acad. Sci. U. S. A.* **96,** 2907–2912
33. El Kharroubi, A., Piras, G., and Stewart, C. L. (2001) *J. Biol. Chem.* **276,** 8674–8680
34. Koishi, K., Zhang, M., McLennan, I. S., and Harris, A. J. (1995) *Dev. Dyn.* **202,** 244–254
35. Cooper, R. N., Tajbakhsh, S., Mouly, V., Cossu, G., Buckingham, M., and Butler-Browne, G. S. (1999) *J. Cell Sci.* **112,** 2895–2901
36. Springer, T., Galfre, G., Secher, D. S., and Milstein, C. (1979) *Eur. J. Immunol.* **9,** 301–306
37. Hirsch, S., and Gordon, S. (1983) *Immunogenetics* **18,** 229–239
38. Choi, J., Costa, M. L., Mermelstein, C. S., Chagas, C., Holtzer, S., and Holtzer, H. (1990) *Proc. Natl. Acad. Sci. U. S. A.* **87,** 7988–7992
39. Rosenblatt, J. D., and Parry, D. J. (1992) *J. Appl. Physiol.* **73,** 2538–2543
40. Yan, Z., DeGregori, J., Shohet, R., Leone, G., Stillman, B., Nevins, J. R., and Williams, R. S. (1998) *Proc. Natl. Acad. Sci. U. S. A.* **95,** 3603–3608
41. Zhang, P., Wong, C., Liu, D., Finegold, M., Harper, J. W., and Elledge, S. J. (1999) *Genes Dev.* **13,** 213–224
42. Eisen, M. B., Spellman, P. T., Brown, P. O., and Botstein, D. (1998) *Proc. Natl. Acad. Sci. U. S. A.* **95,** 14863–14868
43. Helin, K. (1998) *Curr. Opin. Genet. Dev.* **8,** 28–35
44. Megeney, L. A., Kablar, B., Garrett, K., Anderson, J. E., and Rudnicki, M. A. (1996) *Genes Dev.* **10,** 1173–1183

45. Couteaux, R., Mira, J. C., and d'Albis, A. (1988) *Biol. Cell* **62,** 171–182
46. Campbell, W. G., Gordon, S. E., Carlson, C. J., Pattison, J. S., Hamilton, M. T., and Booth, F. W. (2001) *Am. J. Physiol.* **280,** C763–C768
47. Wittwer, M., Fluck, M., Hoppeler, H., Muller, S., Desplanches, D., and Billeter, R. (2002) *FASEB J.* **16,** 884–886
48. Carson, J. A., Nettleton, D., and Reecy, J. M. (2002) *FASEB J.* **16,** 207–209
49. Sreekumar, R., Halvatsiotis, P., Schimke, J. C., and Nair, K. S. (2002) *Diabetes* **51,** 1913–1920
50. Haslett, J., and Kunkel, L. (2002) *Int. J. Dev. Neurosci.* **20,** 359–365
51. Roth, S. M., Ferrell, R. E., Peters, D. G., Metter, E. J., Hurley, B. F., and Rogers, M. A. (2002) *Physiol. Genomics* **10,** 181–190
52. Yang, X., Pratley, R. E., Tokraks, S., Bogardus, C., and Permana, P. A. (2002) *Diabetologia* **45,** 1584–1593
53. Relaix, F., Weng, X., Marazzi, G., Yang, E., Copeland, N., Jenkins, N., Spence, S. E., and Sassoon, D. (1996) *Dev. Biol.* **177,** 383–396
54. Leibovitch, M. P., Solhonne, B., Guillier, M., Verrelle, P., Leibovitch, S. A., and Verrelle, P. (1995) *Oncogene* **10,** 251–260
55. Stewart, C. E., James, P. L., Fant, M. E., and Rotwein, P. (1996) *J. Cell. Physiol.* **169,** 23–32
56. Wolffe, A. P., and Matzke, M. A. (1999) *Science* **286,** 481–486
57. Cossu, G., and Borello, U. (1999) *EMBO J.* **18,** 6867–6872
58. Cossu, G., Tajbakhsh, S., and Buckingham, M. (1996) *Trends Genet.* **12,** 218–223
59. Coutelle, O., Blagden, C. S., Hampson, R., Halai, C., Rigby, P. W., and Hughes, S. M. (2001) *Dev. Biol.* **236,** 136–150
60. Cornelison, D. D., Olwin, B. B., Rudnicki, M. A., and Wold, B. J. (2000) *Dev. Biol.* **224,** 122–137
61. Beauchamp, J. R., Heslop, L., Yu, D. S., Tajbakhsh, S., Kelly, R. G., Wernig, A., Buckingham, M. E., Partridge, T. A., and Zammit, P. S. (2000) *J. Cell Biol.* **151,** 1221–1234
62. Cornelison, D. D., and Wold, B. J. (1997) *Dev. Biol.* **191,** 270–283
63. Reynaud, E. G., Leibovitch, M. P., Tintignac, L. A., Pelpel, K., Guillier, M., and Leibovitch, S. A. (2000) *J. Biol. Chem.* **275,** 18767–18776
64. Reynaud, E. G., Pelpel, K., Guillier, M., Leibovitch, M. P., and Leibovitch, S. A. (1999) *Mol. Cell. Biol.* **19,** 7621–7629
65. Urashima, M., Teoh, G., Akiyama, M., Yuza, Y., Anderson, K. C., and Maekawa, K. (1999) *Br. J. Cancer* **79,** 1032–1036
66. Phelps, D. E., Hsiao, K. M., Li, Y., Hu, N., Franklin, D. S., Westphal, E., Lee, E. Y., and Xiong, Y. (1998) *Mol. Cell. Biol.* **18,** 2334–2343
67. Skapek, S. X., Rhee, J., Spicer, D. B., and Lassar, A. B. (1995) *Science* **267,** 1022–1024
68. DeGregori, J., Kowalik, T., and Nevins, J. R. (1995) *Mol. Cell. Biol.* **15,** 4215–4224
69. Neuman, E., Flemington, E. K., Sellers, W. R., and Kaelin, W. G., Jr. (1994) *Mol. Cell. Biol.* **14,** 6607–6615
70. Ohtani, K., DeGregori, J., Leone, G., Herendeen, D. R., Kelly, T. J., and Nevins, J. R. (1996) *Mol. Cell. Biol.* **16,** 6977–6984
71. Kowalik, T. F., DeGregori, J., Leone, G., Jakoi, L., and Nevins, J. R. (1998) *Cell Growth Differ.* **9,** 113–118